J IRAN CHEM SOC
DOI 10.1007/s13738-013-0383-5

ORIGINAL PAPER

Synthesis, characterization, DNA interaction, thermal and in vitro biological activity investigation of some Ni(II)-Isatin bishydrazone complexes

Mostafa K. Rabia · Ahmad Desoky M. Mohamad · Nabawia M. Ismail · Ali Abdo Mahmoud

Received: 28 August 2013 / Accepted: 16 November 2013

Abstract Complexes of the type [Ni (L) (H_2O)] $Cl_2.nH_2O$, where L = [(pyridine-2-carboxaldhyde)-3-isatin]-bishydrazone (cpish), [(2-acetyl pyridine)-3-isatin]-bishydrazone (apish) and [(2-benzoyl pyridine)-3-isatin]-bishydrazone (bpish) have been synthesized and characterized on the bases of elemental analysis, molar conductance, IR, NMR, electronic spectra and thermal analysis (TGA and DTA). Moreover, the stoichiometry and the formation constants of these complexes have been determined spectrophotometrically. Kinetics and thermodynamic parameters of the thermal decomposition have been computed from the thermal data using Coats and Redfern method, which confirm first-order kinetics. The bioefficacy of the ligands and their complexes have been examined for their in vitro antibacterial and antifungal activity against many types of bacteria and anti fungal cultures, which are common contaminants of the environment in Egypt, and the results indicate that the ligands and their metal complexes possess notable antimicrobial activity. Investigation of their interaction with CT-DNA under physiological conditions, using spectroscopic (UV–visible) and hydrodynamic techniques (viscosity measurements). Binding constant "K_b" obtained from spectroscopic methods revealed significant binding of compounds with DNA via intercalation, Furthermore, free energies of compounds–DNA interactions indicated spontaneity of their binding.

Electronic supplementary material The online version of this article (doi:10.1007/s13738-013-0383-5) contains supplementary material, which is available to authorized users.

M. K. Rabia · A. D. M. Mohamad · N. M. Ismail · A. A. Mahmoud (✉)
Chemistry Department, Faculty of Science, Sohag University, Sohag 82534, Egypt
e-mail: aliabdo@science.sohag.edu.eg; alyabdo8081@yahoo.com

Keywords Isatin-bishydrazone ligands · Ni(II) complexes · Formation constant · Antibacterial · Antifungal · DNA-interaction

Introduction

The study of the interaction of exogenous small molecules with DNA has been the subject of intensive investigation for decades. It provides insight into the screening design of new and more efficient multifarious drugs targeting to DNA for the prevention of diseases and the improvement of the medicinal efficiency. It is evident from the biochemical structure of DNA macromolecule that it has variety of sites where ligands/pro-drug candidates may interact. However, most drugs binding to DNA do not involve covalent bond formation and are thus dependent on intermolecular interactional forces [1]. Hence interactional binding is mostly non-covalent and equilibrated process. There are three key modes of non-covalent drug–DNA interactions: Groove binding, hydrophobic intercalation and non-specific electrostatic surface binding. Nucleic acids are common targets for antiviral, anticancer and antibiotic drugs [2–4]. A concrete knowledge of drugs–nucleic acid interaction, including sequence recognition, structural details, kinetics and thermodynamics of binding [5] is prerequisite for the optimization of drug effectiveness as well as to discover new drugs. The binding interactions of small molecules and their complexes with DNA have attained utmost importance for both therapeutic and scientific reasons [6]. These interactions may also be used for conformational recognition to find new structures of DNA and sequence-specific differences along the helix of DNA molecule [7–9].

The metal ions play key role in the biological processes of life. It has been estimated that about 0.03 % by

Published online: 05 December 2013

weight of human body consists of metals [10]. It was found that concentration of metals like Cd, Cr, Ti, V, Ni, Cu, Se and Zn were lower in cancerous parts of the kidney than in non-cancerous parts [11]. As many medicinal organic compounds do not have a pure organic mode of action and traces of metal ions are required directly or indirectly for their activation. Metal complexes are well known to accelerate the drug action and the efficiency of a therapeutic agent can often be enhanced upon coordination with metal ions [12]. The pharmacological activity has also been found to be highly dependent on the nature of the metal ion and the donor sequence of the ligands as different ligands exhibit different biological properties [13]. Therefore, the chemistry of metal-based drugs (metallopharmaceutical) has a broader role. As a consequence, the investigation of the biological properties of the individual bioactive metal complex drug candidate is of an utmost importance. The identification of metal complex–DNA interaction is of fundamental importance to the understanding of the molecular basis of therapeutic activity.

Among the metal complexes the influence of metal Isatin-hydrazones, especially transition metal Isatin-hydrazones and their derivatives, has received considerable attention owing to their synthetic and effective wide range of biological activity [14–18]. Metal Isatin-hydrazones based drugs have evoked keen interest in the development of coordination chemistry, resulting in an enormous number of publications ranging from pure synthetic work to physiochemical and biochemical relevant studies [19, 20].

One strategy for the development of drugs and chemotherapeutic agents involves medicinal candidates which interact reversibly with DNA through non-covalent interactions. Therefore, the design of new metal Isatin-hydrazones with the ability to bind specifically and bring about DNA cleavage is important to develop new chemotherapeutic agents [21]. Thus, the aim of present work is to design and characterize novel Ni(II) complexes with newly synthesized Isatin-bishydrazones ligands. Testing the in vitro antibacterial and antifungal activity of the free ligands and their complexes against many types of bacteria and anti fungal cultures, which are common contaminants of the environment in Egypt, in order to assess the antimicrobial activity of the synthesized compounds. Make an attempt to investigate the interaction of the Ni(II) Isatin-bishydrazone complexes with (CT-DNA) using UV–visible spectroscopy, and hydrodynamic technique under physiological conditions [at stomach (4.7) and blood (7.4) pH and at body temperature (37 °C)].

The structures of the prepared ligands and their Ni(II) complexes in this investigation are shown in Scheme (1).

Experimental

Chemicals

All chemicals were used as received without further purification. Isatin, 2-acetyl pyridine, 2-benzoyl pyridine and pyridine-2-carboxaldhyde were obtained from Sigma-Aldrich Company Ltd. Hydrazine hydrate and hydrated Nickel chloride ($NiCl_2.6H_2O$) was obtained from BDH Company. All other reagents and solvents (methanol, ethanol and DMF) were purchased from commercial sources and were of analytical grade.

Synthesis of the ligands and there Ni(II)-complexes

Synthesis of the ligands

Isatin-bishydrazone ligands, namely [(pyridine-2-Carboxaldhyde)-3-isatin]-bishydrazone (cpish), [(2-acetyl pyridine)-3-isatin]-bishydrazone (apish) and [(2-benzoyl pyridine)-3-isatin]-bishydrazone (bpish) were prepared in two steps: the first step is the synthesis of Isatin-monohydrazone, followed by condensation with the 2-pyridyl, giving the Isatin-bishydrazone Ligands.

Synthesis of Isatin-monohydrazone Isatin (1.47 g, 10 mmol) was dissolved in methanol (40 mL) and was added to a solution of hydrazine hydrate (0.05 g, 10 mmol) dissolved in hot methanol (5 mL). The resulting mixture was refluxed for 3 h on a water bath. On cooling, the formed yellow compound was filtered, washed with cold methanol, dried and recrystallized from methanol [22].

Synthesis of Isatin-bishydrazone ligands A (1.0 mmol of 2-pyridyl (2-acetyl pyridine or 2-benzoyl pyridine or Pyridine-2-carboxaldhyde) was added drop wise to a hot methanolic solution of Isatin-monohydrazone (1.0 mmol), the resulting mixture was refluxed for 1 h with constant stirring and then 2–3 drops of glacial acetic acid was added, with continued refluxing for 4 h under constant magnetic stirring. On cooling, the formed ligand was filtered, washed with cold methanol, dried, and finally recrystallized from methanol.

Synthesis of Ni(II) complexes

A solution of the metal salt in minimum amount of water [$NiCl_2.6H_2O$, 1.0 mmol] was added drop wise to a hot

Scheme 1 Schematic diagram of the Isatin-bishydrazone ligands and their Ni(II) complexes

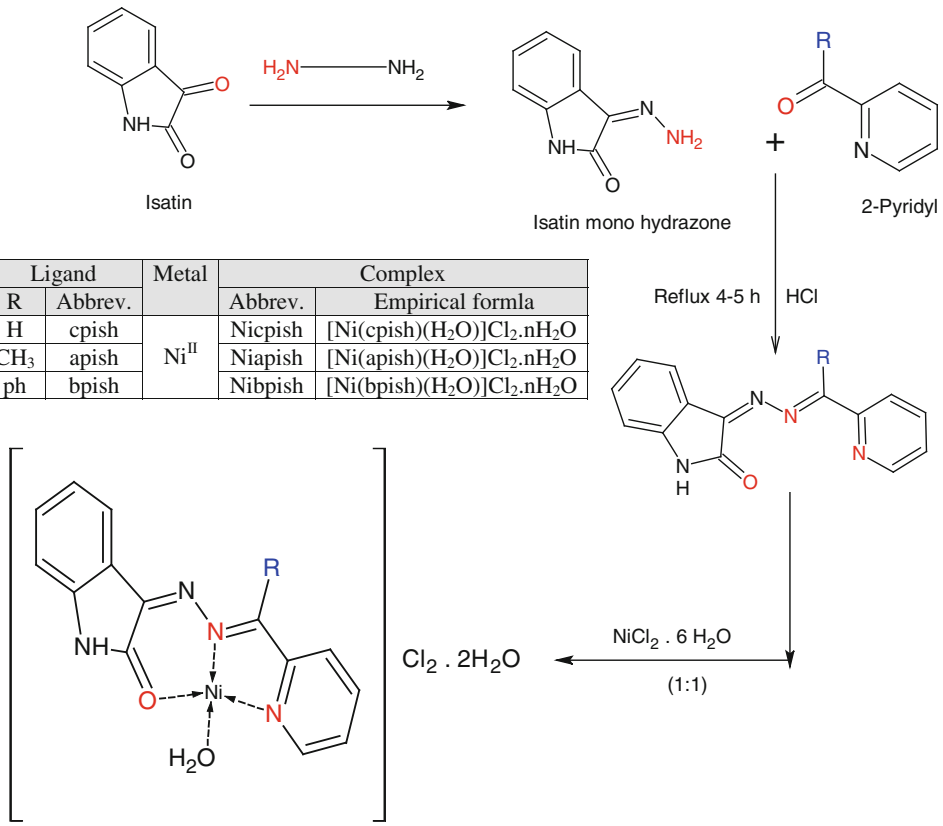

Ligand		Metal	Complex	
R	Abbrev.		Abbrev.	Empirical formla
H	cpish	Ni^{II}	Nicpish	$[Ni(cpish)(H_2O)]Cl_2.nH_2O$
CH_3	apish		Niapish	$[Ni(apish)(H_2O)]Cl_2.nH_2O$
ph	bpish		Nibpish	$[Ni(bpish)(H_2O)]Cl_2.nH_2O$

methanolic solution of the ligand [cpish or apish or bpish, 1.0 mmol]. The resulting mixture was refluxed at 70 °C for 10 h under constant stirring. By evaporation overnight, the resulted solid product was filtered, washed with water–methanol solvent, dried and finally recrystallized from water–methanol mixed solvent.

Analyses of the complexes

The stoichiometric analysis (C, H and N) of the new compounds was performed using elemental analyzer Perkin-Elmer model 40c, at the Micro-analytical Centre at Cairo-University, Egypt. The molar conductance of 10^{-3} molar dilution was measured by JENWAY conductivity-meter model 4320 at 298 K at wide range of different solvents to verify the complex structure. The IR spectra were recorded on Shimadzu FTIR model 8101 in the region 4,000–400 cm^{-1} using dry KBr discs. The electronic spectra of the new compounds in methanol were recorded in the region of 200–800 nm using a 10-mm matched quartz cells on Jasco UV–Visible spectrophotometer model V-530. ^{1}H NMR and ^{13}C NMR spectra were recorded in DMSO-d_6 solvent (solvent peak = 3.8 ppm) on a Bruker Advance 400 instrument. Rigaku model 8150 thermo-analyzer was used for simultaneous recording of TG–DTA curves at a heating rate of 10 min^{-1}.

Biological activity

In Vitro antibacterial and anti-fungi screening

The antimicrobial activity of all the synthesized Isatin-bishydrazone ligands and their corresponding Ni(II) complexes were tested against six bacterial (three gram positive bacteria and three gram negative bacteria) and six fungal strains. These strains are common contaminants of the environment in Egypt, some of which are involved in human and animal diseases (Trichophyton rubrum, Candida albicans, Geotrichum candidum, Scopulariopsis brevicaulis, Aspergillus flavus and Staphylococcus aureus (+ve)) or in plant diseases (Fusarium oxysporum) or frequently reported from contaminated soil, water and food substances [Escherichia coli (−ve), Bacillus cereus (+ve), Pseudomonas aeruginosa (−ve), Serratia marcescens (−ve) and Micrococcus luteus (+ve)]. To prepare inocula for bioassay, bacterial strains were individually cultured for 48 h in 100-ml conical flasks containing 30 ml nutrient broth medium. Fungi were grown for 7 days in 100-ml conical flasks containing 30 ml Sabouraud's dextrose broth. Bioassay was done in 10-cm sterile plastic Petri plates in which microbial suspension (1 ml/plate) and 15 ml of appropriate agar medium (15 ml/plate) were poured. Nutrient agar and Sabouraud's dextrose agar were, respectively, used for bacteria and fungi. After

solidification of the media, 5-mm diameter cavities were cut in the solidified agar (3 cavities/plate) using sterile cork borer. Chemical compounds dissolved in dimethyl sulfuxide (DMSO) at 100 ppm were pipetted in the cavities (20 ul/cavity). Cultures were then incubated at 28 °C for 48 h in case of bacteria and up to 7 days in case of fungi. Results were read as the diameter (in mm) of inhibition zone around cavities.

Determination of minimum inhibitory concentration (MIC) value

To determine the minimum inhibitory concentrations (MICs), chemical compounds giving positive results were diluted with DMSO to prepare a series of descending concentrations down to 5 ppm. Diluted chemicals were similarly assayed as mentioned before and the least concentration (below which no activity) was recorded as the MIC.

Determination of the Activity Index (%) for the complexes

The antibacterial and antifungal activities of a common standard antibiotic Chloramphenicol as antibacterial standard and Clotrimazole as antifungal standard were also recorded maintaining the same protocol as above at the same concentrations and solvent. The antibacterial and antifungal results of the compounds were compared with the standard and % Activity Index for the complexes was calculated using the formula as under [23]:

$$\%\text{Active index} = \frac{\text{Zone of inhibition by test compound (diamter)}}{\text{Zone of inhibition by compound (diamter)}} \times 100$$

Interaction with Calf Thymus DNA (CT-DNA)

Spectroscopic titrations

The purity of DNA was tested spectrophotometrically; CT-DNA solution at pH 7.4 gave a ratio of UV absorbance at 260 and 280 nm of about >1.86:1, indicating that the DNA was sufficiently free from protein contamination [24, 25] and fit for use. Concentration of DNA determined spectrophotometerically at 260 nm (using $\varepsilon_{260} = 6{,}600\ \text{mol}^{-1}\ \text{cm}^2$) was found to be 1.056×10^{-4} M. The stock solution was stored at 4 °C and used within only 1 day. Spectrophotometric titrations as optical probes were carried out at stomach pH (4.7) and blood pH (7.4), and at body temperature 37 °C, using 0.1 M acetate and 0.1 M phosphate buffers, respectively. The UV–Vis. absorption spectra were recorded by keeping the concentration of each compound constant (10 μM), while varying the concentration of CT-DNA from 8 μM up to 35 μM in the sample cell by standard addition method. In order to achieve the equilibrium between the compound and DNA for the formation of compound–DNA adduct, solutions were allowed to stay for 5 min at 37 °C before each measurement was made.

Viscosity measurements

Initially viscosity of DNA solution (η_o) was determined at pH; 7.4, 4.7, and at 37 °C. Then specific viscosity contribution (η) due to the DNA (8 μM) in the presence of increasing concentration of the investigated compound was determined. Viscosity measurements were carried out using an Ostwald type viscometer, thermostated at 37 ± 1 °C. The flow times of the samples were repeatedly measured with an accuracy of ±0.2 with a digital stopwatch operated timer for different concentrations of the complex (2–20 μM), maintaining the concentration of DNA constant (8 μM).

Results and discussion

Identification of the prepared compounds

Microanalysis and molar conductance measurements

The results of the microanalysis of the prepared Isatin-bishydrazone ligands and their Ni(II) complexes in addition to the molar conductance measurements (Table 1), suggested that the subject ligands act as neutral tridentate and form complexes in 1:1 molar ratio (metal to ligand), with 1:2 electrolytic nature of all the complexes [26, 27]. Thus, the general formula of the prepared complexes is suggested to be $[Ni(L)(H_2O)]Cl_2.nH_2O$ according to the following reaction:

$$NiCl_2.6H_2O + L \rightarrow [Ni(L)(H_2O)]Cl_2.2H_2O,$$

where L is the Isatin-bishydrazone ligand. The satisfactory results of analytical data (Table 1) and spectral studies revealed that the ligands and their complexes were of good purity.

Spectroscopic studies

Spectra and mode of bonding In the absence of a powerful technique such as single X-ray crystallography, infrared spectra has proven to be the most suitable technique to give enough information to elucidate the nature of bonding of the subject ligands to the metal ion. Thus a detailed interpretation of IR spectra of the free ligands and the effect of binding of Ni(II) of the vibration frequencies of the free ligands are discussed to determine the

Table 1 Analytical and physical data of ligands and their complexes

	Empirical formula (formula weight)	Color	m.p (°C)	Yield (%)	Elemental analysis found (calculated)					μ_v (Ω^{-1} Cm^2 mol^{-1})		
					C %	H %	N %	Cl %	M %	Methanol	DMF	Ethanol
cpish	$C_{14}H_{10}N_4O$ (250.255)	Red	245 °C	89	67.19 (67.20)	4.03 (4.33)	22.39 (22.30)	–	–	–	–	–
Ni- cpish complex	[Ni (cpish) H_2O]Cl_2 .$2H_2O$ (433.89)	Dark brown	>300	65	38.84 (38.75)	3.49 (3.72)	12.94 (12.91)	16.38 (16.34)	13.56 (13.53)	170	140	85
apish	$C_{15}H_{12}N_4O$ (264.28)	Red	250 °C	85	68.17 (68.50)	4.58 (4.25)	21.20 (20.98)	–	–	–	–	–
Ni- cpish complex	[Ni (apish)H_2O]Cl_2 .$2H_2O$ (447.93)	Dark brown	>300	60	40.31 (40.22)	3.83 (4.05)	12.54 (12.51)	15.87 (15.83)	13.13 (13.10)	166	137	82
bpish	$C_{20}H_{14}N_4O$ (326.35)	Red	265 °C	85	73.61 (73.55)	4.32 (4.28)	17.17 (17.05)	–	–	–	–	–
Ni- cpish complex	[Ni(bpish) H_2O]Cl_2 .$2H_2O$ (509.99)	Dark brown	>300	70	47.29 (47.10)	3.57 (3.95)	11.03 (10.99)	13.96 (13.90)	11.55 (11.51)	160	133	80

coordination sites which may involve in chelation. The significant infrared bands of the subject ligands and their metal complexes are given in Table 2. The observed bands may be classified into those originating from the ligands and those arising from the bonds formed between metal ions and the coordinating sites. The IR spectrum of the Isatin-bishydrazone ligands exhibited characteristic band due to (-NH) and lactonyl carbon ν(C=O) at ≈3,180–3,200 cm^{-1} and ≈1,722 cm^{-1} [28], respectively. In addition, the strong band at ≈1,460 cm^{-1} and a characteristic high-intensity band at ≈1,621 cm^{-1} in the IR spectrum of the Isatin-bishydrazone ligands are assigned to ν(C=N) and ν(HC=N), respectively. In comparison with the spectra of the Isatin-bishydrazone ligands, all the Ni(II) complexes exhibited the band of ν(HC=N) in the region ≈1,590 cm^{-1}; showing the shift of the band to lower wave numbers indicating that the azomethine nitrogen is coordinated to the metal ion [29, 30]. The band of ν(C=O) in the region 1,670–1,680 cm^{-1} in the metal complexes showing the shift to lower wave numbers confirms that the carbonyl oxygen is coordinated to the metal ion [31, 32]. The unaltered position of a band due to ν(NH) and ν(C=N) in all the metal complexes indicates that these groups are not involved in coordination. The new bands in the region of 500–510 and 630–650 cm^{-1} in the spectra of the complexes are assigned to stretching frequencies of (M–N) and (M–O) bonds, respectively [33]. Thus the IR spectral results provide strong evidences for the complexation of Isatin-bishydrazone ligands with metal ion in tridentate mode via Isatin-carbonyl(C=O), azomethine-N(C=N), and pyridine-N (C=N).

NMR spectra The NMR spectra data provide valuable information regarding the structure of Isatin-hydrazone ligands. The ^{1}H-NMR and ^{13}C-NMR spectra of the Isatin-bishydrazone ligands (in DMSO-d_6) were recorded using tetramethylsilane as the internal standard.

^{1}H-NMR and spectra The ^{1}H-NMR spectrums of the ligands are summarized in Table 3. In ^{1}H-NMR, the singlet signal at ≈10.8–11.0 ppm corresponds to the -NH proton of Isatin. The azomethine proton appeared as singlet peak at ≈8.98 ppm in the case of cpish-ligand and disappeared in the other ligands (apish and bpish) due to substitution of the azomethine proton by methyl or phenyl group in apish and bpish ligands, respectively. Also, all the eight aromatic protons (Isatin ring and pyridine ring) appeared as a multiplet in the range ≈7.80–8.20 ppm. Protons of the methyl group in the case of apish ligand appeared at ≈2.37 ppm as singlet. Also the five aromatic protons of the substituted phenyl ring appeared as multiplet in the range ≈7.80–8.20 ppm in the case of bpish-ligand.

Table 2 The infrared absorption frequencies (cm^{-1}) and electronic spectra of the investigated Isatin-hydrazone ligands and their metal complexes

No	Compound	υ (OH)[a]	υ (N–H)[b]	υ (C=O)[c]	υ (HC=N)[d]	υ (C=N)[e]	υ (M–O)	υ (M–N)	Electronic spectra		
									λ_{max}, nm	ε_{max} (dm^3 mol^{-1} cm^{-1})	Assignment
1	cpish	3421.2	3276.5	1721.7	1613.7	1460.3	–	–	237	1744.05	π–π^*
									324	865.49	n–π^*
2	Ni- cpish	3430.8	3287.1	1685.0	1611.7	1409.0	656.8	510.2	627 nm	320.12	d–d band
									676 nm	293.02	d–d band
3	apish	3393.2	3180.0	1721.7	1618.5	1458.4	–	–	254	538.30	π–π^*
									274	580.97	π–π^*
									325	339.05	n–π^*
4	Ni- apish	3357.5	3159.8	1672.5	1592.4	1463.2	637.6	504.4	625 nm	723.22	d–d band
									680 nm	256.57	d–d band
5	bpish	3424.0	3181.0	1721.7	1607.9	1452.6	–	–	252	1096.47	π–π^*
									271	882.56	π–π^*
									327	653.87	n–π^*
6	Ni- bpish	3359.4	3160.7	1671.5	1594.4	1463.2	636.6	503.5	636 nm	268.80	d–d band
									682 nm	295.95	d–d band

[a] Vibrations of the water molecules

[b] Vibrations of the Indol ring (N–H)

[c] Vibrations of the Lactonyl group (C=O)

[d] Vibrations of the azomethine group (C=N)

[e] Vibrations of group from the β-hydrazone of Isatin (C=N)

^{13}C NMR spectra The ^{13}C-NMR spectrum of the Ligands and its DEPT-^{13}C-NMR are summarized in Table 3. In ^{13}C-NMR; the azomethine carbon appears as singlet peak at ≈149–154 ppm in all the ligands, and still as it is in the DEPT-NMR in the case of cpish-ligand and disappeared in the DEPT-NMR of the apish, bpish ligands due to substitution of methyl and phenyl groups in the apish, bpish ligands respectively.

Electronic spectra Electronic spectra are a valuable tool for coordination chemists to draw important information about the structural aspects of the complexes. The ligands, which are organic compounds, have absorption bands in the ultraviolet region and in some cases these bands extend to higher wavelength region due to conjugation. Upon complexation with metal ions, changes will take place in the electronic properties of the system. New bands in the visible region due to d–d absorption and charge transfer spectra from metal to ligand (M → L) or ligand to metal (L → M) can be observed and these data can be processed to obtain information regarding the structure and geometry of the complexes. The Electronic spectra of the Isatin-bishydrazone ligands and its Ni(II)-complexes were recorded in MeOH (≈1 × 10^{-3} mol/dm^3) in the range 200–800 nm at 298 K. The absorption maxima bands are listed in Table 2 and the spectra are given in Fig. 1. The UV–Vis spectrum of the Isatin-bishydrazone ligand shows important strong bands at ≈388 and ≈230 nm due to π–π^* and n–π^* transitions [34], respectively. These bands are altered to a greater extent on complexation. The spectrum of Ni(II)-complexes shows characteristic band at λ_{max} = 670–680 nm due to d–d transition band.

Stoichiometry and stability of the complexes

Determination of the stoichiometry of the complexes

The stoichiometry of the various Ni(II) Isatin-bishydrazone complexes was determined by applying the spectrophotometric molar ratio [35–37] and continuous variation [38, 39] methods, which suggested the possible formation of 1:1 complexes. The curves of continuous variation method (Fig. 2) displayed maximum absorbance at mole fraction × ligand = 0.5, indicating the formation of the complex between the metal ion and the ligands in 1:1 (metal:ligand) molar ratio as presented in Scheme 1. Moreover, the data resulted from applying the mole ratio method support the same metal ion to ligand ratio of the prepared complexes (cf. Fig. 3).

Table 3 NMR Spectroscopic data of the Isatin-hydrazone ligands

Compound	^{1}H-NMR spectra		^{13}C-NMR spectra		DEPT ^{13}C-NMR
	Chemical Shift (δ, ppm)	Assignment	Chemical Shift (δ, ppm)	Assignment	Chemical Shift (δ, ppm)
cpish ($C_{14}H_{10}N_4O$)			164.5	C=O	–
	11.25	(S, 1H, NH-group)	157.4	β-hydrazone of Isatin (C=N).	–
	8.85	(S, 1H, CH-azomethine)	153.6	C=N Pyridine ring	–
	6.80–8.20	(m, 8H, Aromatic)	152.3	–CH=N azomethine	–
			148.5	=C–NH	152.3
			110–146	8-CH aromatic	110–146
apish ($C_{15}H_{12}N_4O$)			162.3	C=O	–
	10.70	(S, 1H, NH-group)	155. 5	β-hydrazone of Isatin (C=N).	–
	–	(S, 1H, CH-azomethine)	150.2	C=N Pyridine ring	–
	6.70–8.50	(m, 8H, Aromatic)	149.3	–C=N azomethine	–
	1.85	(s, 3H, methyl)	147.5	=C–NH	–
			110–146	8-CH aromatic	110–146
			18.9	–CH_3 group	18.9
bpish ($C_{20}H_{14}N_4O$)			165.1	C=O	–
		(S, 1H, NH-group)	156.3	β-hydrazone of Isatin (C=N).	–
	11.15	(S, 1H, CH-azomethine)	155.5	C=N Pyridine ring	–
	–	(m, 13H, Aromatic)	153.7	–C=N azomethine	–
	6.75–8.40		150.5	=C–NH	–
			110–149	13-CH aromatic	110–149

Evaluation of the apparent formation constants of the synthesized complexes

The formation constants (K_f) of the studied Ni(II) Isatin-bishydrzone complexes formed in solution were obtained from the spectrophotometric measurements by applying the continuous variation method according to the following relations [40]:

$$K_f == \frac{A/A_m}{\left(1 - A/A_m\right)^2 C},$$

where A_m is the absorbance at the maximum formation of the complex, A is the actual absorbance of the complex and C is the initial concentration of the metal. As mentioned in Table 4, the obtained K_f values indicate the high stability of the prepared complexes. The values of K_f for the studied complexes increase in the following order: Ni-bpish > Ni-apish > Ni-cpish.

Thermal investigation of the prepared Isatin-bishydrazone complexes

T. G, Dr. T. G analysis of the prepared Isatin-bishydrazone complexes

The importance of this study on the Ni(II) complexes of the Isatin-bishydrazone ligands stems from their possible biological activities. Therefore, they are widely subjected to investigation by thermal analysis and other physico-chemical methods, and also for perfect deduction of the complex structure, by determining the number of hydrated and coordinated water molecules. Thermal data of the complexes are given in Table 5. The Ni (II) complexes of the Isatin-bishydrazone ligands exhibited thermal stability in the range ≈25–50 °C and then degraded in three steps (Fig. 4a, b, c). The first degradation step in the temperature range ≈350–360 K may account for the loss of the hydrated water molecules (two water molecules). The second degradation step in the temperature range ≈470–540 K may be attributable to the loss of the coordinated water molecule (one water molecule) and the third step of decomposition occurs within the temperature range ≈730–790 K, corresponding to the loss of organic moiety leaving $NiCl_2$ as metallic residue.

Kinetics of thermal decomposition of the complexes

The kinetic analysis parameters such as activation energy (ΔE^*), enthalpy of activation (ΔH^*), entropy of activation (ΔS^*), and free energy change of decomposition (ΔG^*) were evaluated graphically by employing the Coats–Redfern relation [41]:

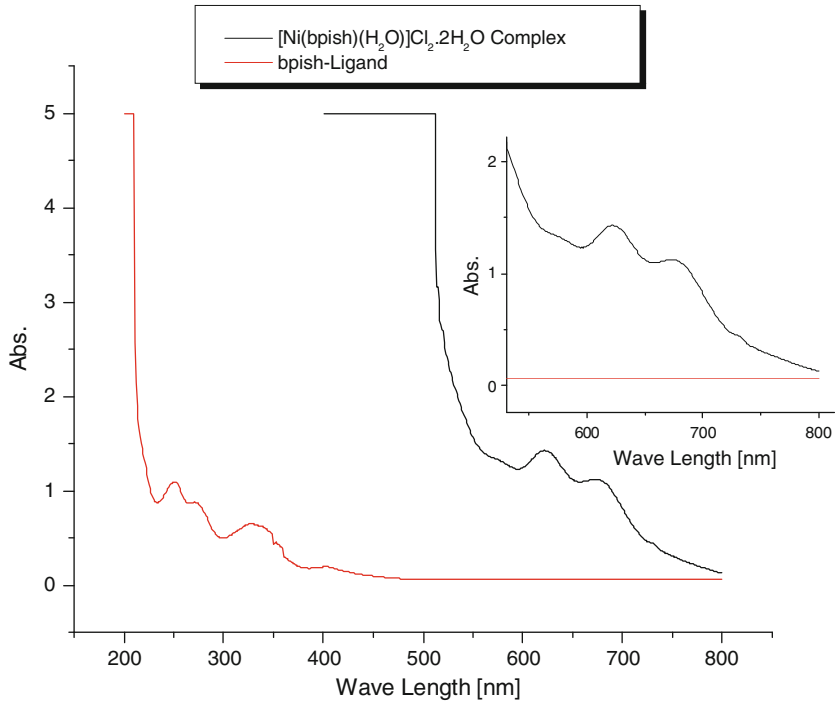

Fig. 1 UV–Vis. Spectrum of the Ni(II) Isatin-hydrazone complexes

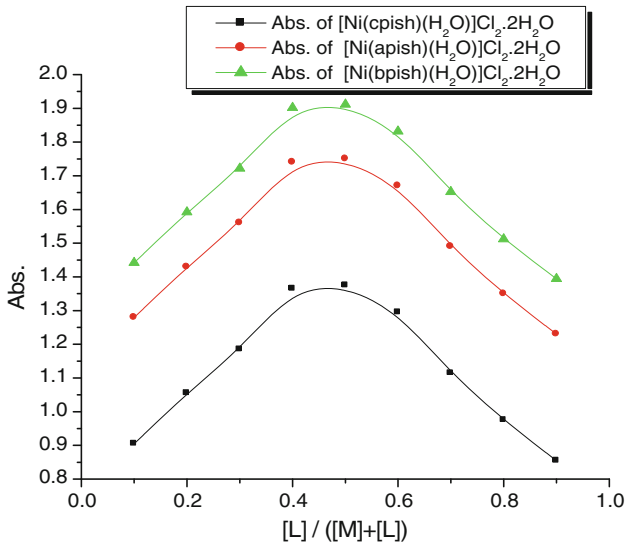

Fig. 2 Continuous variation plot of Ni(II)-Isatin-bishydrazone complexes

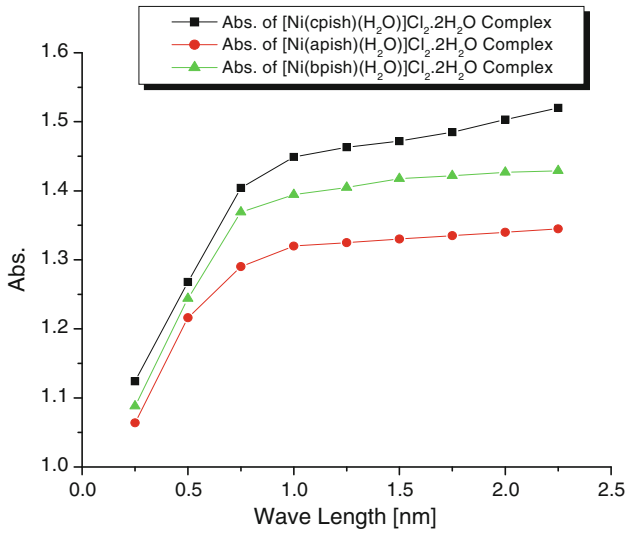

Fig. 3 Molar ratio plot of Ni(II)-Isatin-bishydrazone complexes

$$\mathrm{Log}\left[\frac{-\mathrm{Ln}(1/(1-\alpha))}{T^2}\right] = \mathrm{Log}\left[\frac{AR}{\beta E^*}\left(1-\frac{2RT}{E^*}\right)\right] - \frac{E^*}{2.303RT},$$

where α is the fraction of sample decomposed at temperature T, R the gas constant, E^* the activation energy in J mol^{-1}, β the linear heating rate and $(1 - 2RT/E^*) = 1$. A plot of left-hand side of Coats–Redfern equation against 1/T gives a slope from which E^* was calculated and A (Arrhenius constant) was determined from the intercept. Figure 5 represents the linear plot in case of Ni(II) complexes. The Coats and Redfern linearization plots confirmed first-order kinetics for the decomposition process. The activation entropy (ΔS^*), the activation enthalpy (ΔH^*), and the free energy of activation (ΔG^*) can be calculated using the following equations [42, 43]:

$$\Delta S^* = 2.303\ R\ \log\left[\left(\frac{Ah}{K_B T_s}\right)\right],$$

$$\Delta H^* = E_a - RT_S$$

$$\Delta G^* = \Delta H^* - T\Delta S^*$$

where h, K_B and T_s are Planck constant, Boltzmann constant and the peak temperature obtained from the DTA curve, respectively. The calculated values of E^*, ΔS^*, ΔH^* and ΔG^* for the decomposition steps are given in Table 6. According to the kinetic data obtained from the TG curves, all the complexes have negative entropy, which indicate that the complexes are formed spontaneously. The negative entropy also indicates a more ordered activated state that may be possible through the decomposition of other products. The negative values of the entropies of activation are compensated by the values of the enthalpies of activation, leading to almost the same values for the free energies of activation [44]. The high values of the activation energies reflected the thermal stability of the complexes. The positive values of $\Delta H^{\#}$ reflected the endothermic nature of thermal decomposition. Furthermore, the negative values of $\Delta S^{\neq}$ in the studied complexes indicate that the reaction rates were slower than normal and the positive values of $\Delta G^{\neq}$ indicated the non-spontaneous nature of the process. The data clearly indicates similarity in the thermal degradation of the complexes.

Biological activity (anti-bacteria and antifungal activity)

The susceptibilities of certain strains of bacteria and fungal cultures to Isatin-bishydrazone complexes were evaluated by measuring the diameter (in mm) of the inhibition zone around cavities. The antimicrobial activity data of all synthesized Isatin-bishydrazone ligands and there Ni(II) complexes are summarized in Tables 7 and 8 and show that the newly synthesized ligands and their Ni(II) complexes possess notable biological activity. The antibacterial screening results exhibited marked enhancement in activity on coordination with the metal ions against most the testing bacterial strains (cf. Figs. 6, 7). This enhancement in the activity can be rationalized to the basis of the structures of the ligands by possessing an additional azomethine (C=N) linkage which is important in elucidating the mechanism of transamination and resamination reaction in biological system [45]. It has also been suggested that the ligands with nitrogen and oxygen donor systems might inhibit enzyme production [46], since the enzymes which require these groups for their activity appear to be especially more susceptible to deactivation by the metal ions upon chelation [47]. The polarity of the metal ion is reduced by chelation [48] and this mainly because of the partial sharing of its positive charge with the donor groups and possibly with the delocalized π-electrons within the whole chelation ring, which is formed because of the coordination. This process of chelation increases the lipophilic nature of the central metal atom, which in turn favors its permeation through the lipoid layer of the membrane [49]. This is also responsible for the increasing of the hydrophobic character and liposolubility of the molecules in crossing the cell membrane of the microorganism and hence enhances the biological utilization ratio and activity of the testing drug/compound. The results are quite promising. It is evident from the results that the biological activity of the metal complexes is higher than the corresponding ligands. This enhancement in the activity of the metal complexes can be explained on the basis of chelation theory [50]. It is, however, known that the chelating tends to make the Schiff base act as more powerful and potent bactereostatic agents, thus inhibiting the growth of bacteria and fungi more than the parent

Table 4 The formation constant (K_f), stability constant (pK) and Gibbs free energy ($\Delta G^{\neq}$) values of the prepared complexes in aqueous-methanol at 298 K

Complex	Type of the complex	Formation constant (K_f)	Stability constant (Log K_f)	$\Delta G^{\neq}$ (KJ/mol)
Ni-cpish complex	1:1	4.09×10^9	9.61	−54.8212
Ni-apish complex	1:1	4.47×10^9	9.65	−55.0321
Ni-bpish complex	1:1	5.43×10^9	9.73	−55.5348

Table 5 Thermo analytical data. (TG, DTG)

Complex	Step	TG_{range} (°C)	DTA_{max} (°C)	Thermal effect	Mass loss: Obs. (Calc.) (%)	Assignment	Metallic residue
Ni-cpish complex	I	53.11–106.55	78.38	Endo	8.98 (8.30)	$2H_2O$ (hydrated)	$NiCl_2$
	II	106.55–426.69	209.42	Endo	5.13 (4.14)	$1H_2O$ (coordinated)	
	III	426.69–600.53	506.16	Endo	58.10 (57.68)	Organic moiety	
Ni-apish complex	I	54.07–219.16	78.71	Endo	8.55 (8.03)	$2H_2O$ (hydrated)	$NiCl_2$
	II	219.16–389.07	196.61	Endo	5.22 (4.02)	$1H_2O$ (coordinated)	
	III	389.07– 497.8	460.33	Endo	75.11 (72.86)	Organic moiety	
Ni-bpish complex	I	56.07–210.55	87.68	Endo	7.35 (7.06)	$2H_2O$ (hydrated)	$NiCl_2$
	II	210.55–404.91	265.57	Endo	4.05 (3.53)	$1H_2O$ (coordinated)	
	III	404.91–580.93	519.39	Endo	65.78 (63.99)	Organic moiety	

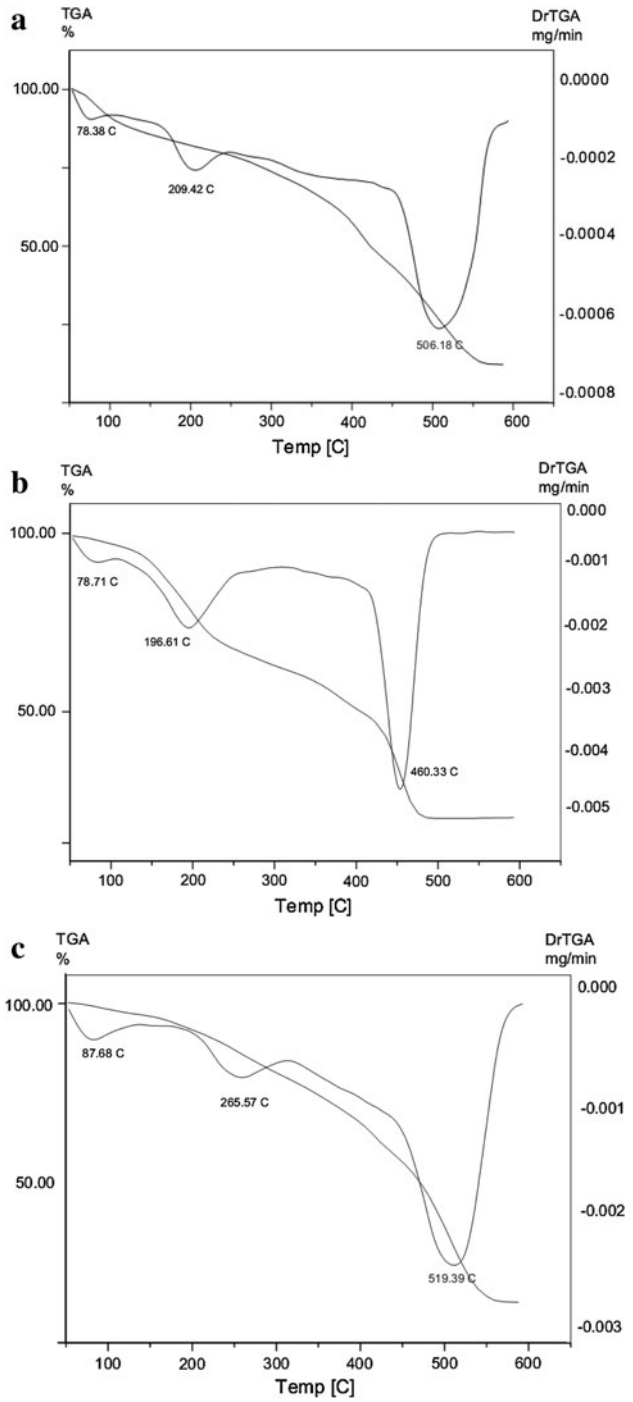

Fig. 4 Thermal decomposition of **a** Ni-cpish, **b** Ni-apish and **c** Ni-bpish

ligand [51–53], and also noticed that the activity of Ni(II) complexes were more than the parent ligands.

DNA binding study by UV–Vis. spectroscopy

The binding of complex to DNA has been characterized classically through absorption titrations [54]. Generally,

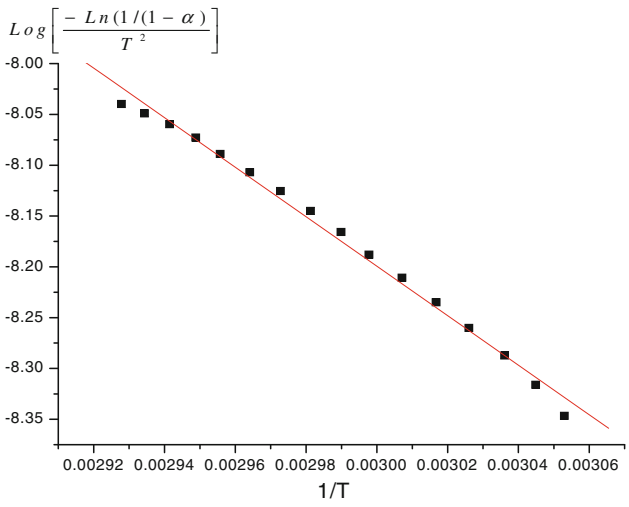

Fig. 5 Coats–Redfern linear plot for [Ni (cpish)(H2O)]Cl2.2H2O complex

hypochromic (red shift) or hyperchromic effect (blue shift) are observed in the absorption spectra of small molecules if they intercalate with DNA [55]. Spectrophotometric studies of Isatin-bishydrazone complexes were carried out under physiological pH 4.7(stomach) and 7.4 (blood) and body temperature 37 °C. No significant change in the wave-lengths was observed at both pHs, which may indicate non-interactive behavior of these compounds with buffer solutions. UV–Vis. spectra of Isatin-bishydrazone complexes were recorded separately after addition of DNA and the effect of the varying concentrations of DNA on optimized concentrations (10 μM) of all the compounds in stomach (Fig. 8a, b, c) and blood pH (Fig. 9a, b, c) under body temperature. Peak intensity in the absorption spectra of Isatin-bishydrazone complexes (Ni-cpish, Ni-apish and Ni-bpish complexes) increased with a pronounced red shift of 5.0, 4.0 and 6.0 nm, respectively, at stomach pH, (Fig. 8a, b, c), and increased with a pronounced blue shift of magnitude 7.0, 9.0 and 8.0 nm, respectively, at blood pH (Fig. 9a, b, c), by the addition of DNA. Percent decrease in the peak intensities of Isatin-bishydrazone complexes in the presence of DNA was calculated as 28.8, 37.17 and 23.37 %, respectively, at stomach pH, while percent increase was calculated as 62.33, 39.08 and 23.55 %, respectively, at blood pH, using the following equation:

$$H\% = \frac{A_{\text{free}} - A_{\text{bound}}}{A_{\text{free}}} \times 100$$

A peculiar hypochromism, (Fig. 8a, b, c) and hyperchromism (Fig. 9a, b, c) indicate the interaction of electronic states of intercalating chromophores of the compounds and those of the stacked base pairs of CT-DNA [56]. A red shift can be directly linked with π*-orbital of

Table 6 Thermodynamic activation parameters for the thermoanalysis of the investigated Isatin-hydrazone complexes

Complex	Order	Step	E^* (KJ mol^{-1})	A (S^{-1})	ΔS^* (JK^{-1} mol^{-1})	ΔH^* (KJ mol^{-1})	ΔG^* (J mol^{-1})
Ni-cpish complex	1	I	49.255	494,185.73	−137.29	46.333	94.576
		II	8.386	124,409.39	−151.40	4.375	77.414
		III	12.859	127,856.08	−155.15	6.381	127.275
Ni-apish complex	1	I	51.593	496,722.47	−137.26	48.669	96.945
		II	43.955	53,371.46	−158.21	40.051	114.350
		III	136.150	390,861.98	−145.36	130.053	236.652
Ni-bpish complex	1	I	40.780	53,708.27	−155.967	37.782	94.036
		II	40.254	11,163.51	−172.363	35.776	128.606
		III	61.315	13,620.96	−173.920	54.727	192.539

Table 7 Antibacterial activity of the synthesized Isatin-hydrazone ligands and their metal complexes

Compound conc. (ppm)		Diameter of inhibition zone in mm, minimum inhibition concentration (MIC) and Activity Index (%) for some bacteria																	
		Gram-positive bacteria									Gram-negative bacteria								
		Staphylococcus aureus (+ve)			*Micrococcus luteus (+ve)*			*Bacillus cereus (+ve)*			*Escherichia coli (−ve)*			*Pseudomonas aeruginosa (−ve)*			*Serratia marcescens (−ve)*		
		mm	MIC	%	mm	MIC	%	mm	MIC	%	Mm	MIC	%	mm	MIC	%	mm	MIC	%
cpish	100	6	45	40	5	50	35.7	10	40	45.4	9	50	45	5	45	25	7	50	38.8
apish	100	4	40	26.7	6	45	42.8	9	55	40.9	8	45	40	7	50	35	9	55	50
bpish	100	5	50	33.3	7	40	50	8	45	36.4	7	45	35	8	50	40	6	50	33.3
Ni-cpish	100	13	20	86.7	10	15	71.4	17	20	77.3	16	25	80	17	20	85	12	30	66.7
Ni-apish	100	12	25	80	11	20	78.6	14	20	63.6	15	25	75	15	15	75	12	25	66.7
Ni-bpish	100	11	25	73.3	10	25	71.4	15	15	68.2	16	20	80	15	25	75	10	25	55.6
Chloramphenicol as antibacterial standard		15		100	14		100	22		100	20		100	20		100	18		100

mm, diameter of inhibition zone in mm; MIC, minimum inhibition concentration (ppm); %, Activity Index

Table 8 Anti-fungi activity of the synthesized Isatin-hydrazone ligands and their metal complexes

Compound conc. (ppm)		Diameter of inhibition zone in mm, minimum inhibition concentration (MIC) and Activity Index (%) for some fungi																	
		Candida albicans			*Geotrichum candidum*			*Trichophyton rubrum*			*Fusarium oxysporum*			*Scopulariopsis brevicaulis*			*Aspergillus flavus*		
		mm	MIC	%	mm	MIC	%	mm	MIC	%	Mm	MIC	%	mm	MIC	%	mm	MIC	%
cpish	100	6	40	42.8	6	55	30	10	40	33.3	8	30	44.4	11	40	45.8	12	45	40
apish	100	5	50	35.7	5	45	25	9	30	30	7	35	38.9	9	50	37.5	9	55	30
bpish	100	5	55	35.7	7	50	35	9	35	30	5	40	27.8	7	45	29.2	8	40	26. 7
Ni-cpish	100	11	30	78.6	13	25	65	20	20	66.7	15	30	83.3	18	20	75	19	30	63.3
Ni-apish	100	10	25	71.4	13	30	65	19	20	63.3	16	25	88.9	19	20	79.2	20	20	66. 7
Ni-bpish	100	11	25	78.6	14	25	70	21	25	70	14	20	77.8	18	25	75	22	15	73.3
Clotrimazole as antifungal standard		14		100	20		100	30		100	18		100	24		100	30		100

mm, diameter of inhibition zone in mm, MIC, minimum inhibition concentration (ppm), %, Activity Index

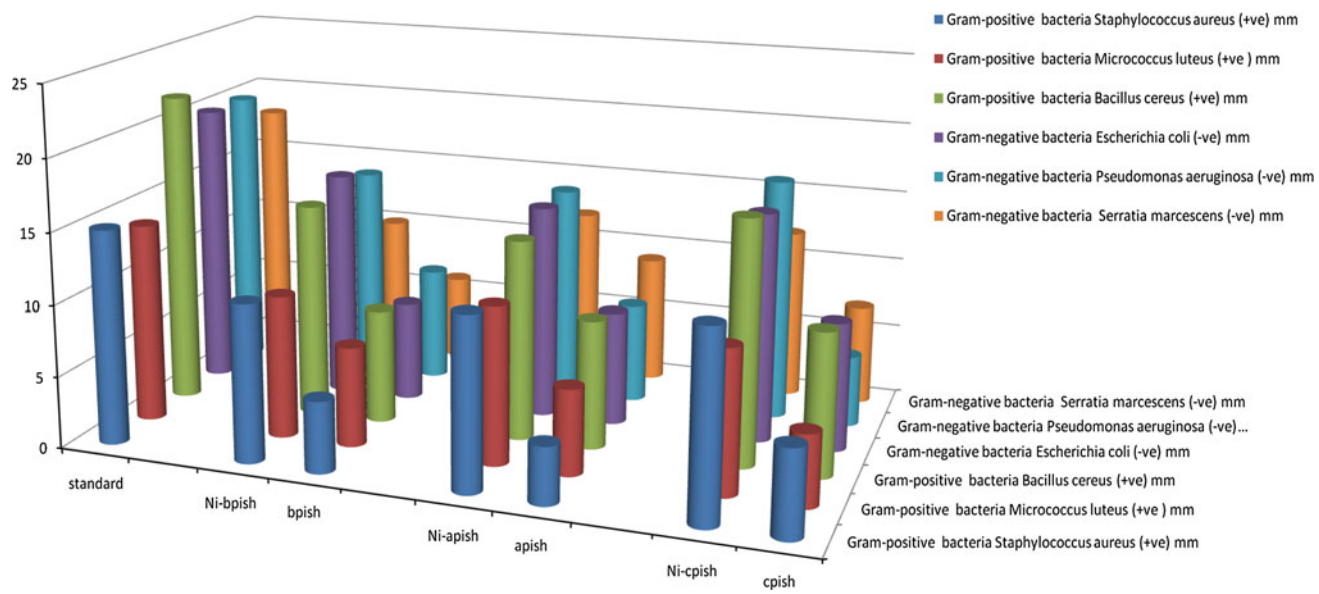

Fig. 6 Antibacterial activity of the synthesized Isatin-hydrazone ligands and their Ni(II) complexes

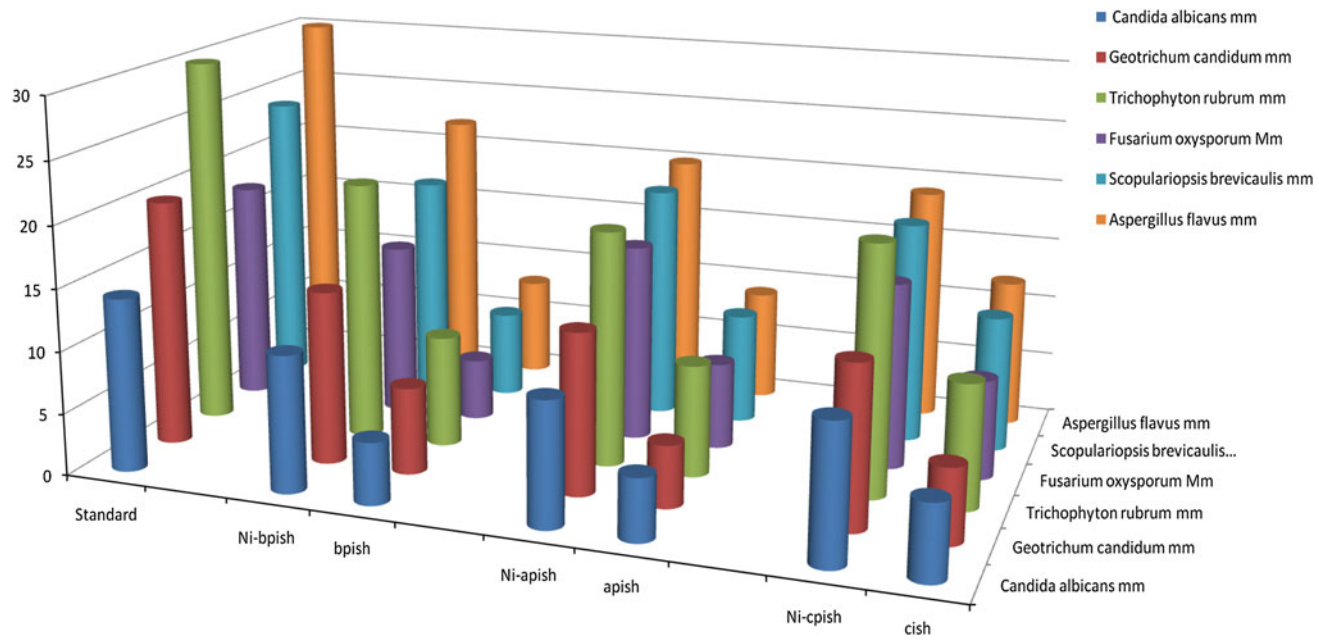

Fig. 7 Antifungal activity of the synthesized Isatin-hydrazone ligands and their Ni(II) complexes

intercalated compound couples with the π-orbital of the base pairs, thus decreasing π–π* transition energy. On the other hand, the coupling π-orbital is partially filled by electrons, thus decreasing transition probabilities and concomitantly resulting in hypochromism [57]. A blue shift may also be attributed to improper coupling (due to conformational changes) of π*-orbital of intercalated ligand with the π-orbital of the base pairs. This unstacking of base pairs (distortion in the π-orbital of the base pairs and π*-orbital of intercalated ligand) infatuate slight blue shift (hypsochromic effect). Similarly reduction of face to face base stacking (exposed electrons) induces enhancement of absorption intensity (hyperchromism) [58–62]. Furthermore, the spectral changes both at stomach and blood pH 4.7, 7.4 were characterized by one isosbestic point for the complexes on titration with DNA; hence the presence of species other than free and the intercalated complexes could be ruled out. The presence of isosbestic point indicates that there is equilibrium between bound DNA and free form of the metal complexes [63–65].

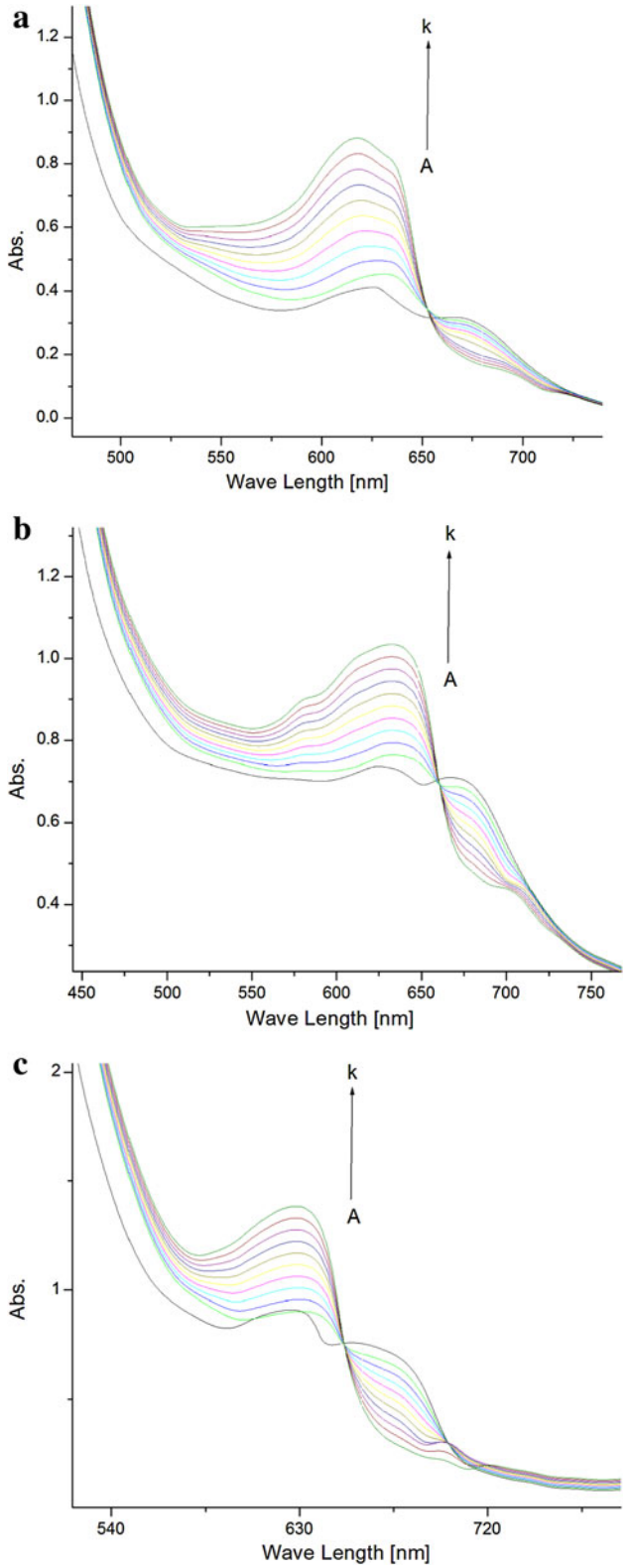

Fig. 8 UV-spectra for **A** Ni-cpish, **B** Ni-apish and **C** Ni-bpish (10×10^{-6} μM) in the absence (a) and presence of 8 μM (b), 11 μ M (c), 14 μM (d), 17 μM (e), 20 μM (f), 23 μM (g), 26 μM (h), 29μ M (i), 32 μM (j), and 35 μM (k) DNA at pH 4.7 and 37 °C. The *arrow direction* indicates increasing concentrations of DNA

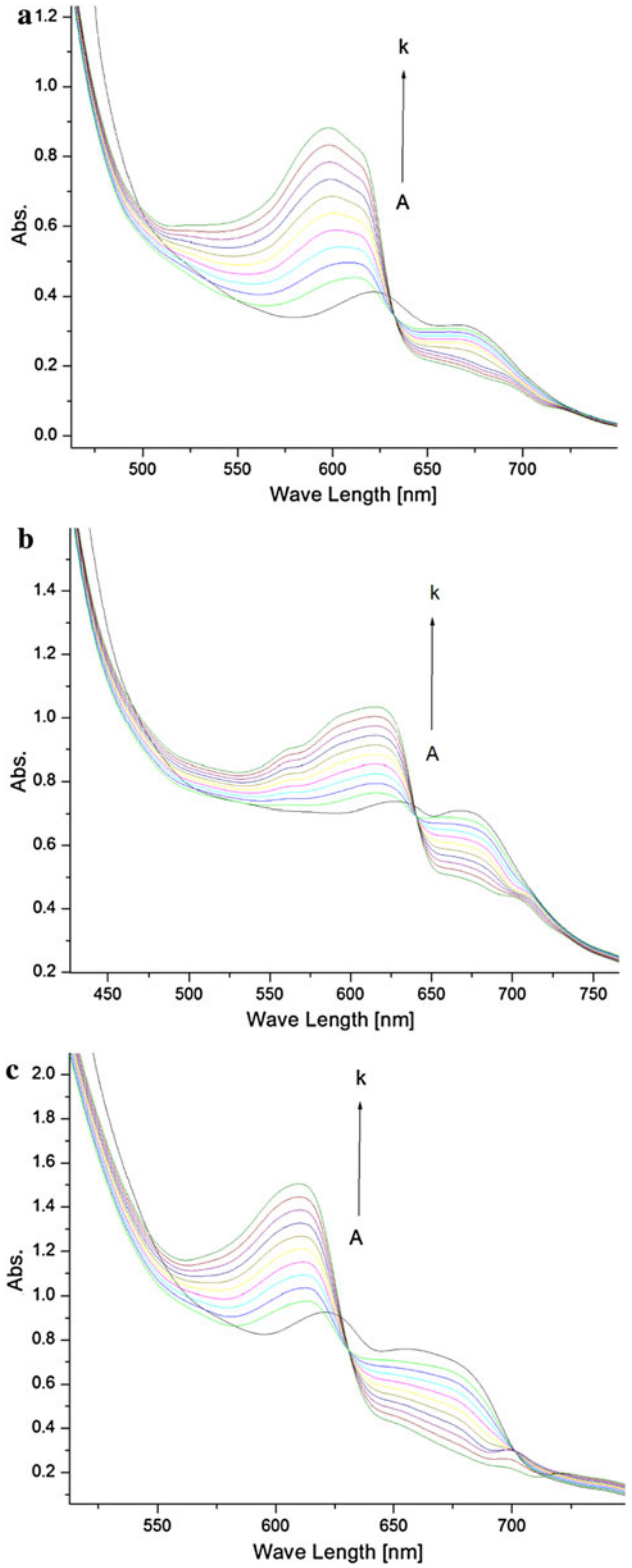

Fig. 9 UV-spectra for **A** Ni-cpish, **B** Ni-apish and **C** Ni-bpish (10×10^{-6} μM) in the absence (a) and presence of 8 μM (b), 11 μ M (c), 14 μM (d), 17 μM (e), 20 μM (f), 23 μM (g), 26 μM (h), 29μ M (i), 32 μM (j), and 35 μM (k) DNA at pH 7.4 and 37 °C. The *arrow direction* indicates increasing concentrations of DNA

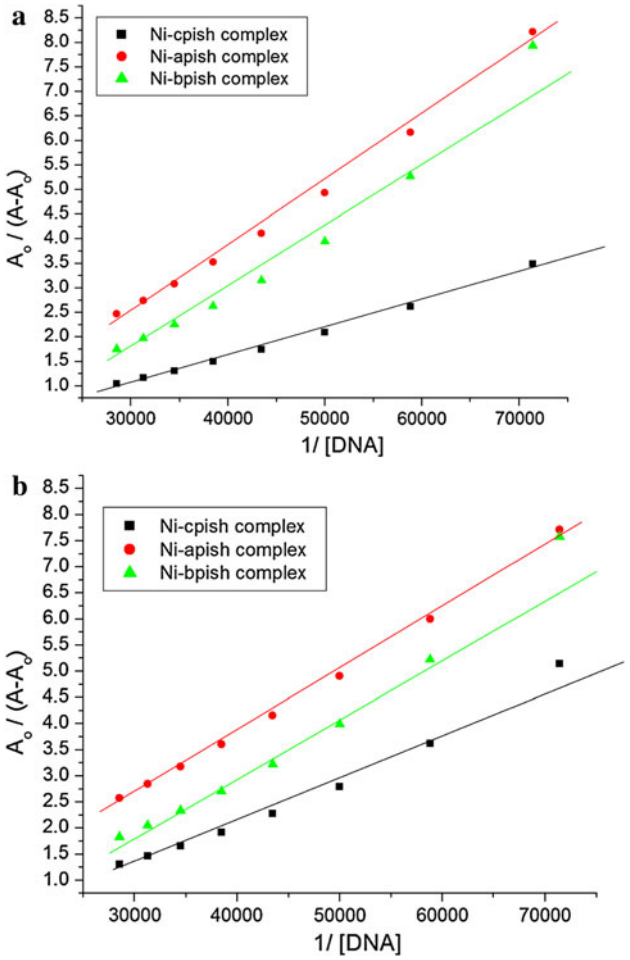

Fig. 10 Plot of Ao/A/Ao vs. 1/[DNA] for the application of Benesi–Hildebrand equation for calculation Ni-cpish, Ni-apish and Ni-bpish – DNA binding constant of at pH **a** 4.7 and **b** 7.4 (37 °C)

Determination of binding constants and free energies by UV–vis. spectroscopy

Since absorbance is varied after addition of CT-DNA, the binding constant "K_b" of the investigated compounds–DNA complexes can be determined from the variation in absorbance in UV–Vis. spectra. The binding constant values were evaluated for these compounds at both pH i.e., 4.7 and 7.4 and at body temperature using Benesi–Hildebrand equation [66–68]:

$$\frac{A_0}{A - A_0} = \frac{\varepsilon_G}{\varepsilon_{H-G} - \varepsilon_G} + \frac{\varepsilon_G}{\varepsilon_{H-G} - \varepsilon_G} \frac{1}{K_b[DNA]},$$

where A_o and A are the absorbances of free compound and DNA bound complex, respectively, ε_G and $\varepsilon_{H\text{-}G}$ the molar extinction coefficients of free compound and DNA bound complex, respectively. From the plot of $A_o/(A - A_o)$ to 1/[DNA], the ratio of the intercept to the slope gave the value of binding constant "K_b", (Fig. 10a, b). The binding constant values of all the compounds were calculated and given in Table 9. K_b values for all the compounds were in the range of 10^3–10^4 M^{-1}. The overall binding constant values are comparable to that of typical intercalators such as isoxazocucu-mine (6.3×10^3 M^{-1}) and lumazine (1.74×10^4 M^{-1}) [69, 70] and revealed stronger interaction of investigated compounds with DNA via intercalation at both pH values. UV–Vis. spectral changes (hypochromic effect with bathochromic shift and hyperchromic effect with hypsochromic shift) also lend support the possibility of intercalative binding mode of interaction.

From the values of binding constant, K_b, and free energy "ΔG" of compound–DNA complex was calculated, using

$$\Delta G = -RT \ln K_b$$

Binding constants are measures of compound–DNA complex stability while free energy indicates the spontaneity/non-spontaneity of compound–DNA binding. Free energies of all the compounds at both pHs were evaluated as negative values showing the spontaneity of compounds–DNA interaction (Table 9).

Viscosity measurements

Viscosity measurement is a comprehensive method to understand the interactional mode between small

Table 9 Spectral parameters for DNA interaction with the prepared complexes: Binding constants and free energy values for compound–DNA complexes from UV–spectrophotometric data at pH 4.7 and 7.4 and at body temperature (37 °C)

	λ_{max} free (nm)	λ_{max} bound (nm)	$\Delta\lambda$	chromism (%)	Type of cheomism	Binding constant K_b (M^{-1})	Free energy ΔG (KJ mol^{-1})
At pH 4.7							
Ni-cpish	627 676	632	5.0	28.8	Hypo	1.14×10^4	−24.08
Ni-apish	625 680	629	4.0	37.17	Hypo	1.2×10^4	−24.23
Ni-bpish	636 682	642	6.0	23.37	Hypo	1.87×10^4	−25.36

Table 9 continued

	λ_{max} free (nm)	λ_{max} bound (nm)	$\Delta\lambda$	chromism (%)	Type of cheomism	Binding constant K_b (M^{-1})	Free energy ΔG (KJ mol^{-1})
At pH 7.4							
Ni-cpish	627		7	62.33	Hyper	1.59×10^4	−24.93
	676						
Ni-apish	625	616	9	39.08	Hyper	7.89×10^3	−23.13
	680						
Ni-bpish	636	628	8	23.55	Hyper	1.69×10^4	−25.09
	682						

Hypo hypochromism, *Hyper* hyperchromism

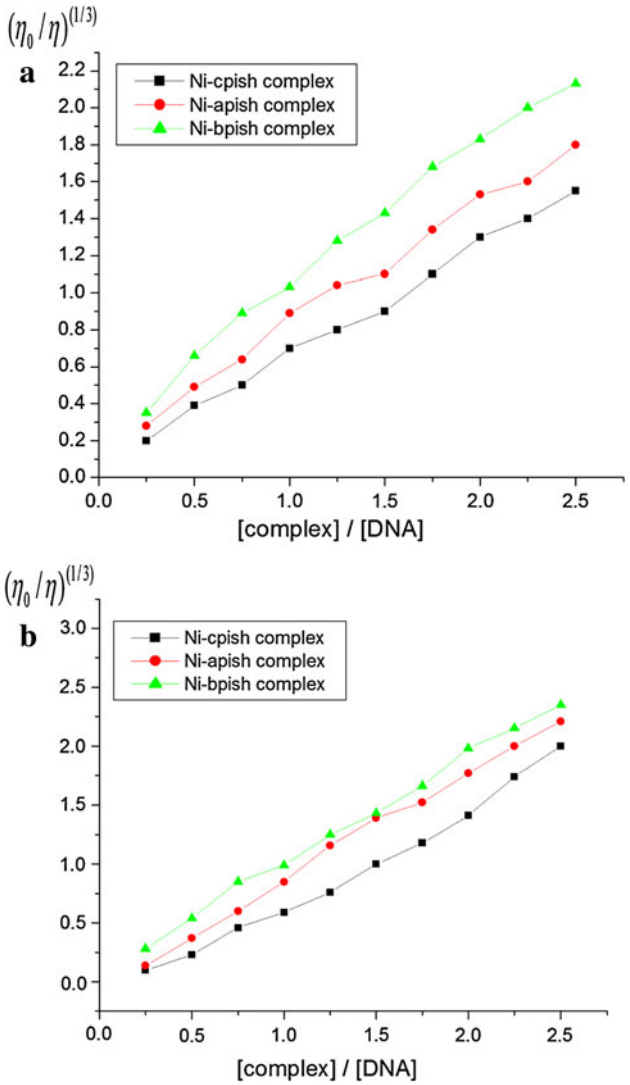

Fig. 11 Plot of relative specific viscosity vs. [Compound]/[DNA] for Ni-cpish, Ni-apish and Ni-bpish at **a** pH 4.7; **b** 7.4 and at 37 °C

molecules and DNA [71]. Lengthening of DNA helix as a consequence of base pair separation to accommodate the binding molecule will lead to an increase in DNA viscosity and is a prerequisite for classical intercalation model [72–74]. Compound–DNA interactions investigated by spectroscopic method in present studies were further verified by viscommetric studies. The third root of values of the relative specific viscosities (η/η_o) for the ligands and the complexes, i.e., $(\eta/\eta_o)^{1/3}$ were plotted against r, where η and η_o are the specific viscosity contributions of DNA in the presence and absence of compounds under investigations and r = [Compound]/[DNA] (Fig. 11a, b). Upon increasing ratio of the compound to DNA, the viscosity of DNA is increasing, which indicated that compound binds to DNA by intercalation of the aromatic rings into the base pairs of DNA [75, 76]. This increase in viscosity is not only the indication of intercalative binding mode but also foreshadows the pronounced hyperchromism, hypochromism, bathochromism and hypsochromism of the complex in the presence of DNA [77].

Conclusion

In this paper, we synthesized and characterized new Ni(II) isatin hydrazone complexes by studying their antimicrobial effect against many types of bacteria and anti fungal cultures, which are common contaminants of the environment in Egypt. The results indicate that the newly synthesized ligands and their Ni(II) complexes possess notable biological activity and exhibited marked enhancement in activity on coordination with the metal ions against the testing bacterial strains. Also, studying the interaction of the new complexes with CT-DNA at physiological conditions. The binding constant values of all the compounds were in the range of 10^3–10^4 M^{-1} by comparing to that of typical intercalators such as isoxazocucu-mine (6.3×10^3 M^{-1}) and lumazine (1.74×10^4 M^{-1}) revealed stronger interaction of investigated compounds with DNA via intercalation at both pH values.

References

1. A. Serganov, D.J. Patel, The Royal Society of Chemistry, Cambridge, 2006), pp. 233–252
2. M. Maiti, G.S. Kumar, J. Nucleic Acids **2010**, 1–23 (2010)
3. M.J. Waring, Annu. Rev. Biochem. **50**, 159–192 (1981)
4. L.H. Hurley, Biochem. Soc. Trans. **29**, 692–696 (2001)
5. N. Arshad, U. Yunus, S. Razzque, M. Khan, S. Saleem, B. Mirza, N. Rashid, Eur. J. Med. Chem. **47**, 452–461 (2012)
6. L. Jia, P. Jiang, J. Xu, Z. Hao, X. Xu, L. Chen, J. Wu, N. Tang, Q. Wang, J.J. Vittal, Inorg. Chim. Acta **363**, 855–865 (2010)
7. J.H. Griffin, P.B. Dervan, J. Am. Chem. Soc. **109**, 6840–6842 (1987)
8. J.K. Barton, Science **233**, 727–734 (1986)
9. E. Palecek, M. Fojta, Anal. Chem. **73**, 74A–83A (2001)
10. S.K. Bharti, S.K. Singh, Int. J. Pharm. Tech. Res. **1**, 1406–1420 (2009)
11. R.A. Sanchez-Delgado, K. Lazardi, L. Rincon, J.A. Urbina, A.J. Hubert, A.N. Noels, J. Med. Chem. **36**, 2041–2043 (1993)
12. V. Kumar, T. Ahamad, N. Nishat, Eur. J. Med. Chem. **44**, 785–793 (2009)
13. V. Zelenak, K. Gyoryova, D. Mlynarcik, Met. Based Drugs **8**, 269–274 (2002)
14. R.W. Daisley, V.K. Shah, J. Pharm. Sci. **73**, 407 (1984)
15. S.N. Pandeya, D. Sriram, E. Declecq, C. Pannecouque, M. Mitvrouw, Indian J. Pharm. Sci. **60**, 207 (1999)
16. S.N. Pandeya, J.R. Dimmock, Pharmazie **48**, 659 (1993)
17. R. Boon, Antiviral Chem. Chemother. **8**, 5 (1997)
18. S.N. Pandeya, D. Siram, G. Nath, E. Declercq, Eur. J. Pharm. Sci. **9**, 25 (1999)
19. N. Hadjiliadis, E. Sletten, in ed. by N. Hadjiliadis, E. Sletten (Eds.), (Blackwell Publishing Ltd., Oxford, 2009) pp. 1–511
20. Z.U. Rehman, A. Shah, N. Muhammad, S. Ali, R. Qureshi, A. Meetsma, I.S. Butler, Eur. J. Med. Chem. **44**, 3986–3993 (2009)
21. R.C. Mehrotra, R. Bohra, *Metal Carboxylates*. (Academic Press Inc., London, 1983)
22. A.D. Kulkarni, S.A. Patil, P.S. Badami, Int. J. Electrochem. Sci. **4**, 717–729 (2009)
23. V.P. Singh, A. Katiyar, Pestic. Biochem. Physiol. **92**, 8–14 (2008)
24. J. Murmur, J. Mol. Biol. **3**, 208–218 (1961)
25. J. Murmur, J. Mol. Biol. **3**, 208–218 (1961)
26. W.J. Geary, Coord. Chem. Rev. **7**, 81 (1971)
27. H.G. olchoubian, O. Nazaria, B.K. ariuki, J. Chin. Chem. Soc., 58(1), (2011)
28. S. Neena, H. Sunita, S. Jyoti, P. Vanita, B.V. Agarwala, Synth. React. Inorg. Met.-Org. Chem. **22**, 1283 (1992)
29. K. Nakamoto, *Infrared spectra of inorganic and coordination compounds* (Wiley-Interscience, New York, 1970)
30. B. Murukan, S.K. Bhageerethi, M. Kochukittan, J. Coord. Chem. **60**(15), 1607 (2007)
31. B. Murukan, S.K. Bhageerethi, M. Kochukittan, J. Coord. Chem. **60**(15), 1607 (2007)
32. G. Cerchiaro, P.L. Saboya, A.M.C. Ferreira, D.M. Tomazela, M.N. Eberlin, Tran. Met. Chem. **29**, 495 (2004)
33. A. Hatzidumitrious, C.A. Bolos, Polyhedron **17**, 1779 (1998)
34. K. Nakamoto, *Infrared spectra of inorganic and coordination compounds* (Wiley-Interscience, New York, 1970)
35. J.H. Yoe, A.L. Jones, Ind. Eng. Chem. (Analyst. Ed.) **16**, 111–115 (1944)
36. R. El-Shiekh, M. Akl, A. Gouda, W. Ali, J. Am. Sci. **7**(4), 797–807 (2011)
37. S.S. Shah, R.G. Parmar, Der Pharma Chemica **3**(1), 318–321 (2011)
38. P. Job, Ann. Chem. **9**, 113–203 (1928)
39. R.M. Issa, A.A. Hassanein, I.M. El-Mehasseb, R.I. El-Abed Wadoud, Spectrochimica Acta Part A **65**, 206–214 (2006)
40. L.H. Abdel-Rahman, R.M. El-Khatib, L.A.E. Nassr, A.M. Abu-Dief, J. Mol. Struct. **1040**, 9–18 (2013)
41. A.W. Coats, J.P. Redfern, Nature **68**, 201–202 (1964)
42. A.A. Abdel Aziz, A.N.M. Salem, M.A. Sayed, M.M. Aboaly, J. Mol. Struct. **1010**, 130–138 (2012)
43. A. Prakash, B.K. Singh, N. Bhojak, D. Adhikari, Spectrochimica Acta Part **A76**, 356–362 (2010)
44. B.K. Singh, R.K. Sharma, B.S. Garg, J. Therm. Anal. Calorim. **84**, 593–600 (2006)
45. N. Nishat, S. Hasnain, S.D. Asma, J. Coord. Chem. **63**(21), 3859–3870 (2010)
46. Z.H. Chohan, C.T. Supuran, A. Scozzafava, J. Enz. Inhib. Med. Chem. **19**, 79–84 (2004)
47. P.G. Avajia, C.H.V. Kumar, S.A. Patilc, K.N. Shivanandad, C. Nagaraju, Eur. J. Med. Chem. **44**(9), 3552–3559 (2009)
48. S.U. Rehman, Z.H. Chohan, F. Naz, C.T. Supuran, J. Enzy. Inhib. Med. Chem. **20**, 333–340 (2005)
49. Z.H. Chohan, M. Arif, Z. Shafiq, M. Yaqub, C.T. Supuran, J. Enz. Inhib. Med. Chem. **21**, 95–103 (2006)
50. K.N. Thimmaiah, W.D. Lloyd, G.T. Chandrappa, Inorg. Chim. Acta. **106**, 81 (1985)
51. A. Kulkarni, P.G. Avaji, G.B. Bagihalli, P.S. Badami, S.A. Patil, J. Coord. Chem. **62**(3), 481 (2009)
52. A.D. Kulkarni, S.A. Patil, P.S. Badami, J. Sulf. Chem., (2009)
53. Z.H. Chohan, H. Pervez, A. Rauf, K.M. Khan, C.T. Supuran, J. Enz. Inhib. Med. Chem. **19**, 417 (2004)
54. A.M. Pyle, J.P. Rehmann, R. Meshoyrer, C.V. Kumar, N.J. Turro, J.K. Barton, J. Am. Chem. Soc. **111**, 3051–3058 (1989)
55. Y. Sun, S. Bi, D. Song, C. Qiao, D. Mu, H. Zhang, Sens. Actuat. B **129**, 799–810 (2008)
56. X. Yang, G.L. Shen, R.Q. Yu, Microchem. J. **62**, 394–404 (1999)
57. Z. Xu, G. Bai, C. Dong, Bioorg. Med. Chem. **13**, 5694–5699 (2005)
58. R.F. Pasternack, E.J. Gibbs, J.J. Vilafranca, Biochemistry **22**, 2406–2414 (1983)
59. S. Mahadevan, M. Palaniandavar, Inorg. Chem. **37**, 693–700 (1998)
60. S. Kashanian, M.B. Gholvand, F. Ahmadi, A. Taravati, A.H. Colagar, Spectrochim. Acta, Part A **67**, 472–478 (2007)
61. A.J. Hobro, M. Rouhi, E.W. Blanch, G.L. Conn, Nucleic Acid Res. **35**, 1169–1177 (2007)
62. J.G. Thomas Jr, Biochim. Biophys. Acta **213**, 417–423 (1970)
63. H.M. Torshizi, T.S. Srivastava, S.J. Chavan, M.P. Chitnis, J. Inorg. Biochem. **48**, 63–70 (1992)
64. A. Blake, A.R. Peacocke, Biopolymers **5**, 871–875 (1967)
65. A.K. Paul, T.S. Srivastava, S.J. Chavan, M.P. Chitnis, S. Desai, K.K. Rao, J. Inorg. Biochem. **61**, 179–196 (1996)
66. G.J. Yang, J.J. Xu, H.Y. Chen, Z.H. Leng, Chin. J. Chem. **22**, 1325–1329 (2004)
67. M.Y. Nie, Y. Wang, H.L. Li, Pol. J. Chem. **71**, 816–822 (1997)
68. X.J. Dang, M.Y. Nie, J. Tong, H.L. Li, J. Electroanal. Chem. **448**, 61–67 (1998)
69. N. Shahabadi, A. Fatahi, J. Mol. Struct. **970**, 90–95 (2010)
70. M.S. Ibrahim, I.S. Shehata, A.A. Al-Nateli, Biomed. Anal. **28**, 217–225 (2002)
71. N.K. Janjua, A. Shaheen, A. Yaqub, F. Perveen, S. Sabahat, M. Mumtaz, C. Jacob, L.A. Ba, H.A. Mohammad, Spectrochim. Acta, Part A **79**, 1600–1604 (2011)
72. N. Shahabadi, A. Fatahi, J. Mol. Struct. **970**, 90–95 (2010)
73. N.K. Janjua, A. Shaheen, A. Yaqub, F. Perveen, S. Sabahat, M. Mumtaz, C. Jacob, L.A. Ba, H.A. Mohammad, Spectrochim. Acta, Part A **79**, 1600–1604 (2011)
74. J.B. Chaires, Energetics of drug–DNA interactions. Biopolymer **44**, 201–215 (1997)

75. N.K. Janjua, A. Shaheen, A. Yaqub, F. Perveen, S. Sabahat, M. Mumtaz, C. Jacob, L.A. Ba, H.A. Mohammad, Spectrochim. Acta, Part A **79**, 1600–1604 (2011)
76. G. Zang, J. Guo, J. Pan, X. Chen, J. Wang, J. Mol. Struct. **923**, 114–119 (2009)
77. X.L. Wang, H. Chao, H. Li, X.L. Hong, Y.J. Liu, L.F. Tan, L.N. Ji, J. Inorg. Biochem. **98**, 1143–1193 (2004)